Anomalous Gray Matter Structural Networks in Major Depressive Disorder

Manpreet K. Singh, Shelli R. Kesler, S.M. Hadi Hosseini, Ryan G. Kelley, Debha Amatya, J. Paul Hamilton, Michael C. Chen, and Ian H. Gotlib

Background: Major depressive disorder (MDD) is characterized by abnormalities in structure, function, and connectivity in several brain regions. Few studies have examined how these regions are organized in the brain or investigated network-level structural aberrations that might be associated with depression.

Methods: We used graph analysis to examine the gray matter structural networks of individuals diagnosed with MDD ($n = 93$) and a demographically similar healthy comparison group ($n = 151$) with no history of psychopathology. The efficiency of structural networks for processing information was determined by quantifying local interconnectivity (clustering) and global integration (path length). We also compared the groups on the contributions of high-degree nodes (i.e., hubs) and regional network measures, including degree (number of connections in a node) and betweenness (fraction of short path connections in a node).

Results: Depressed participants had significantly decreased clustering in their brain networks across a range of network densities. Compared with control subjects, depressed participants had fewer hubs primarily in medial frontal and medial temporal areas, had higher degree in the left supramarginal gyrus and right gyrus rectus, and had higher betweenness in the right amygdala and left medial orbitofrontal gyrus.

Conclusions: Networks of depressed individuals are characterized by a less efficient organization involving decreased regional connectivity compared with control subjects. Regional connections in the amygdala and medial prefrontal cortex may play a role in maintaining or adapting to depressive pathology. This is the first report of anomalous large-scale gray matter structural networks in MDD and provides new insights concerning the neurobiological mechanisms associated with this disorder.

Key Words: Connectivity, depression, graph analysis, gray matter, small world, structural network

Major depressive disorder (MDD) is among the most prevalent and costly of all psychiatric disorders (1). Investigators have documented impairments in MDD in executive function, memory, and emotional processing (2), as well as anomalies in both neural structure and function (3), particularly in the subgenual anterior cingulate cortex (sgACC), dorsolateral prefrontal cortex (DLPFC), ventral striatum, amygdala, and hippocampus (4,5). Importantly, however, findings from these studies of MDD have been equivocal, likely limited by approaches that fail to capture the multivariate structure of abnormalities associated with this complex disorder. Indeed, several lines of evidence suggest that depression is associated with widespread neurobiological difficulties, including atrophy in gray and white matter tissue in areas distributed throughout the brain (6–9), leading investigators to posit that MDD involves alterations in large-scale structural brain networks (10).

In this context, researchers have recently begun to use graph theory to examine brain network organization. Graph theory provides a powerful method for quantifying the organization of brain connectivity, allowing the brain to be depicted as graphs composed of nodes, representing regions or voxels, and edges, representing structural or functional connectivity among the nodes. Graph-theoretical studies have assessed structurally defined networks based on such features as gray matter volume, cortical thickness, surface area, and white matter connections between gray matter regions (11–15). To construct gray matter networks based on structural magnetic resonance imaging (MRI) data, the edges between nodes are defined by the strength of correlation between regional volume measurements (16). Morphometric correlations likely reflect anatomical connectivity (17) and may be influenced by functional connectivity; that is, functional specialization, increased through practice, skill acquisition, and training, can change underlying anatomy (experience-related plasticity). Watts and Strogatz (18) described the concept of small-world networks that have an optimal balance between local specialization and global integration for information processing. Optimal small-world networks have a high level of local clustering (i.e., nodes are often connected to their neighbors), combined with short path lengths (i.e., it takes few steps from any node to any other node in the network), at low network cost (i.e., the mean physical distance between connected nodes is considerably less than is the case in a random network). These and other related metrics can be used to quantify the local density of connections within regions (clustering), the functional integration between regions (path length) (19), and the contribution of strong nodes (hubs) to facilitate global integrative processes.

Three studies using graph analyses with depressed individuals have found aberrations in path length (20,21) and number of connections (degree) (21,22) during sleep and at rest. These studies were limited, however, in examining small samples of participants in their early stages of illness and in assessing disruptions only in functional networks. In the present study, we used graph-theoretical analyses to examine, for the first time, global and regional MRI-derived structural gray matter networks

From the Department of Psychiatry and Behavioral Sciences (MKS, SRK, SMHH, RGK, DA), Stanford University School of Medicine; and Department of Psychology (JPH, MCC, IHG), Stanford University, Stanford, California.

Address correspondence to Manpreet K. Singh, M.D., Stanford University School of Medicine, Department of Psychiatry and Behavioral Sciences, Stanford, CA 94305; E-mail: mksingh@stanford.edu.

Received Nov 8, 2012; revised and accepted Mar 13, 2013.

0006-3223/$36.00
http://dx.doi.org/10.1016/j.biopsych.2013.03.005

in a large sample of adults diagnosed with MDD. Given previous evidence of a diffuse distribution of gray matter atrophy in depression, combined with findings of reductions in small-world characteristics and increased disorganization of functional networks in depressed individuals, we hypothesized that similar anomalies would also characterize structural gray matter networks in MDD. We also examined depression-associated differences in such regional network measures as betweenness (the fraction of short path connections that pass through a particular node), degree, and the contribution of high-degree nodes (i.e., hubs) to the network. Based on previous findings, we hypothesized that, compared with healthy control subjects (HCs), MDD participants would show 1) abnormal network topology, including significant anomalies in clustering and path lengths; 2) lower betweenness and degree; and 3) different hubs from those of HCs and hubs that are centered in key brain regions, including the sgACC, DLPFC, amygdala, and hippocampus.

Methods and Materials

Participants

Ninety-three adults aged 18 to 60 years diagnosed with MDD and 151 age- and gender-comparable HCs were recruited from outpatient psychiatry clinics and through media advertisements. Trained interviewers administered the Structured Clinical Interview for DSM-IV (23), with high interrater reliability (k = .96). Participants were included in the MDD group if they met the DSM-IV criteria for MDD. The HC group consisted of individuals with no current or past Axis I disorder. All participants had 1) no neurologic, psychiatric, or medical conditions known to affect cognitive function (e.g., learning disability, brain injury, psychotic symptoms, bipolar disorder, alcohol or substance abuse); and 2) no physical contraindications for MRI. Fifty-one percent of the MDD participants were taking psychotropic medications at the time of the scan. Finally, participants completed the Beck Depression Inventory-II (24), a self-report measure of depressive symptom severity. This study was approved by the Stanford University Institutional Review Board and all participants provided informed consent.

MRI Data Acquisition and Preprocessing

Magnetic resonance images used in this analysis were aggregated from three scanners (1.5T GE Signa, 3T GE Signa, and 3T GE Discovery; GE Medical Systems, Milwaukee, Wisconsin), all located at the Stanford University Lucas Center for Medical Imaging. Equal proportions of HC and MDD participants with similar demographic characteristics were scanned concurrently at each scanner (76 HC/48 MDD at 1.5T, 60 HC/31 MDD at 3T Signa, 15 HC/14 MDD at 3T Discovery). Spoiled gradient recall pulse sequences had repetition time = 5.9 to 9.6; echo time = 1.1 to 3.4; flip angle = 11, 15, or 17; matrix = 256 × 256; field of view = 220 mm or 250 mm; voxel dimensions = .859 mm × .859 mm; and slice thickness = 1 mm to 1.8 mm. Although investigators have documented reliable voxel-based morphometry data from multiple scanners at various field strengths and pulse sequences at different sites (25), we nevertheless used field strength as a covariate in our analyses.

Image preprocessing was performed using the Statistical Parametric Mapping 8 (SPM; Wellcome Department of Cognitive

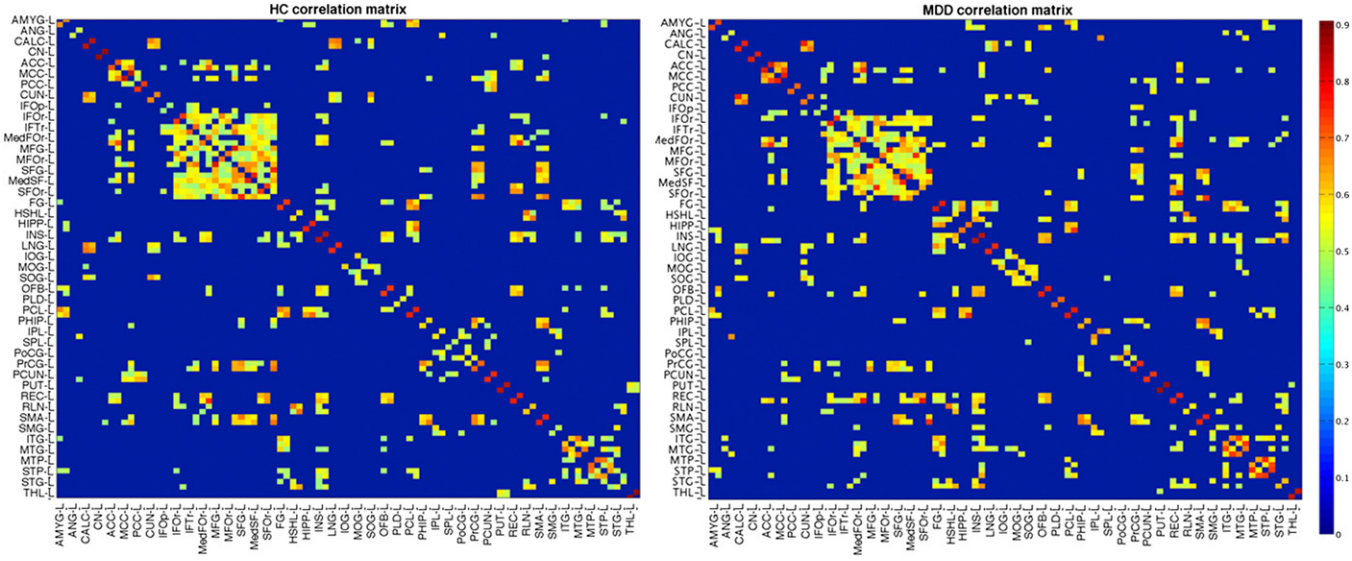

Figure 1. Association matrices. Association matrices for healthy control (HC) and major depressive disorder (MDD) groups; the color-bar shows the strength of the connections. These matrices represent the maps thresholded at the minimum network density (10%) in which the networks of both groups are not fragmented and paths exist between each node and every other node. Correlations below this specified threshold are set to zero. For clarity, only the regions in the left hemisphere are labeled. ACC, anterior cingulate; AMYG, amygdala; ANG, angular gyrus; CALC, calcarine fissure; CN, caudate nucleus; CUN, cuneus; FG, fusiform gyrus; HIPP, hippocampus; HSHL, Heschl's gyrus; IFOp, inferior frontal gyrus, opercular part; IFOr, inferior frontal gyrus, orbital part; IFTr, inferior frontal gyrus, triangular part; INS, insula; IOG, inferior occipital gyrus; IPL, inferior parietal lobule; ITG, inferior temporal gyrus; L, left hemisphere; LNG, lingual gyrus; MCC, mid-cingulate; MedFOr, medial frontal gyrus, orbital part; MedSF, superior frontal gyrus, medial part; MFG, middle frontal gyrus; MFOr, middle frontal gyrus, orbital part; MOG, middle occipital gyrus; MTG, middle temporal gyrus; MTP, middle temporal pole; OFB, olfactory cortex; PCC, posterior cingulate; PCL, paracentral lobule; PCUN, precuneus; PHIP, parahippocampal gyrus; PLD, lenticular nucleus, pallidum; PoCG, postcentral gyrus; PrCG, precentral gyrus; PUT, putamen; REC, gyrus rectus; RLN, rolandic operculum; SFG, superior frontal gyrus; SFOr, superior frontal gyrus, orbital part; SMA, supplementary motor area; SMG, supramarginal gyrus; SOG, superior occipital gyrus; SPL, superior parietal lobule; STG, superior temporal gyrus; STP, superior temporal pole; THL, thalamus.

Neurology, London, United Kingdom) VBM8 toolbox. The images were segmented into gray matter (GM), white matter, and cerebrospinal fluid segments. The GM images were nonlinearly normalized into standard Montreal Neurological Institute space using an age- and gender-adjusted GM study-specific customized template created by the Template-O-Matic (TOM8) toolbox (26,27). Images were then modulated to ensure that relative volumes of GM were preserved following spatial normalization. Sample homogeneity was visually assessed to identify any outliers who were two or more standard deviations of GM volume outside of the sample distributions. Seventeen participants (9 HC, 8 MDD) were excluded for motion artifacts that distorted the boundary between segmented gray and white tissue images.

Region of Interest Extraction

We generated 90 cortical and subcortical regions of interest (ROIs), excluding the cerebellum, from the Automated Anatomical Labeling atlas using the WFU PickAtlas Toolbox (28). The ROIs were identical to those used in previous graph analysis studies of structural correlation networks (12,29). These Automated Anatomical Labeling ROIs were resliced to the same dimension as that of tissue segmented images obtained from the voxel-based morphometry preprocessing step and were subsequently used to mask the individual modulated, normalized GM images and extract the average volume within each ROI using the REX toolbox (http://web.mit.edu/swg/software.htm). A linear regression analysis was conducted at every ROI to control for the effects of age, gender, total brain volume (sum of gray matter, white matter, and cerebral spinal fluid volumes), and scanner field strength. The residuals of this regression were then substituted for the raw ROI volume values and are described as corrected gray matter volumes (15,29,30).

Construction of Structural Correlation Network

The corrected gray matter volumes of all 90 anatomical ROIs were used to construct structural correlation networks. To compute a structural correlation network for each group, a 90×90 association matrix, R, was generated (Figure 1) with each entry, r_{ij}, defined as the Pearson correlation coefficient between corrected gray matter volume measures of regions i and j, across participants (29–31) [partial correlation analysis has been found to underestimate the extent of small-world organization (32)]. From each association matrix, a binary adjacency matrix, A, was derived where a_{ij} was considered 1 if r_{ij} was greater than a specific threshold and zero otherwise. The diagonal elements of the constructed association matrix were also set to zero. The resultant adjacency matrix represented a binary undirected graph, G, in which regions i and j were connected if g_{ij} was unity. Because of methodological challenges in analyzing and comparing weighted networks (33), a graph was constructed with $n = 90$ nodes (anatomical ROIs), with a network degree of E equal to number of edges (links) and a network density (cost) representing the fraction of present connections to all possible connections. Because thresholding the association matrices of different groups at an absolute threshold may yield networks with a different number of nodes and degrees (34), we thresholded the constructed association matrices at a range of network densities (D_{min}: .1: .02: .5) and compared the network topologies across that range (12,29,34). The lower bound of the range was the minimum density in which the networks of both groups were not fragmented (here $D_{min} = .1$). For densities above .5, the graphs became increasingly random (small-world index close to 1).

Network Analyses

Global Network Analyses. We conducted analyses of the constructed structural networks to identify within-group and between-group differences in global network measures such as small-worldness, clustering, and path length. The small-worldness of a complex network has two key metrics: clustering coefficient (C) and characteristic path length (L). The C of a node is a measure of the number of edges between its nearest neighbors, and indexes network segregation. The L of a network is the average shortest path length between all pairs of nodes in the network and is the most commonly used measure of network integration (19). To evaluate the small-world topology of the brain networks, these topological parameters must be benchmarked against corresponding mean values of a null random graph (29,32,33). Thus, the small-world index (SW) of a network is computed as $SW = (C/C_{null})/(L/L_{null})$, where C_{null} and L_{null} are the mean C and L, respectively, of the m (here, $m = 20$) null random networks (18). Clustering coefficient is significantly higher in a small-world network than in random networks (C/C_{null} ratio greater than 1); L is comparable to random networks (L/L_{null} ratio close to 1), resulting in $SW > 1$.

The null networks are typically constructed using rewiring algorithms that preserve the topology of the graphs, i.e., random graphs with the same number of nodes, total edges, and degree distribution as the network of interest (35,36). However, recent evidence suggests that networks constructed from correlations are inherently more clustered than are random networks and that correlation introduces an additive small-world organization to the network (32). To overcome this limitation, we generated null

Table 1. Participant Demographics and Clinical Characteristics

Variable	Group	
	MDD	HC
Female (*n*)	64	96
Male (*n*)	29	55
Mean Age (SD)[a]	38.59 (11.71)	33.08 (10.53)
Mean BDI-II Score (SD)[a]	30.28 (10.17)	2.07 (2.94)
Severity of Current Episode, *n* (%)	85	NA
Mild-moderate	49 (57.6)	
Severe	36 (42.4)	
Mean Age of Onset in Years (SD)	18.26 (10.31)	NA
Number of Depression Recurrences, *n* (%)	74	NA
Single episode – 0 recurrences	4 (5.5)	
One recurrence	10 (13.5)	
Two recurrences	7 (9.4)	
3+ recurrences	53 (71.6)	
Comorbidities, *n* (%)		
Dysthymia (double depression)	7 (7.5)	0 (0)
Panic disorder	6 (6.4)	0 (0)
Social phobia	11 (11.8)	0 (0)
Obsessive-compulsive disorder	3 (3.2)	0 (0)
Posttraumatic stress disorder	9 (9.6)	0 (0)
Current Medications, *n* (%)	91	0 (0)
0 medications	45 (49)	0 (0)
1 medication	24 (26)	0 (0)
2 medications	11 (12)	0 (0)
3+ medications	11 (12)	0 (0)
Number of Weeks Exposed to Medications, Mean (SD)	13.6 (29)	0 (0)

BDI-II, Beck Depression Inventory-II; HC, healthy control; MDD, major depressive disorder; NA, not applicable.

[a] $p = .001$.

networks from covariance matrices that were matched to the distributional properties of the observed covariance matrix using the Hirschberger-Qi-Steuer algorithm (32,37). In addition, we compared the MDD and HC groups on nonnormalized measures of clustering and path length.

Regional Network Analyses. We examined the nodal characteristics of the constructed structural networks to identify group differences in regional network measures. Nodal betweenness and degree were calculated for each of the anatomical ROIs. Nodal betweenness is defined as the fraction of all shortest paths in the network that pass through a given node and is used to detect important anatomical or functional connections. Nodes that bridge disparate parts of the network have a high betweenness (38). In contrast, nodal degree is defined as the number of connections that a node has with the rest of the network and is considered a measure of interaction of a node, structurally or functionally, with the network (39). The quantified nodal betweenness and degree were normalized by the mean network betweenness and degree, respectively, and were then compared between groups (29,30,40).

Hubs are crucial components for efficient communication in a network, providing regulation of information flow and play a key role in network resilience to insult (19). We considered a node to be a hub if its degree was at least one standard deviation higher than the mean network degree (19,29). The regional network and hub analyses were conducted on networks thresholded at the minimum density of full connectivity.

Comparing Network Measures between Groups. A nonparametric permutation test with 1000 repetitions was conducted to test the statistical significance of depression-associated differences in global and regional network topologies (41,42). In each repetition, the corrected regional GM volumes of each participant were randomly reassigned to one of the two new groups with the same number of participants as were in the original diagnostic groups. Then, an association matrix was obtained for each randomized group. The binary adjacency matrices were then estimated by thresholding the association matrices at a range of network densities. The network measures were then calculated for all the networks at each density, and differences between the new randomized groups (at each network density) were computed, resulting in a permutation distribution of difference under the null hypothesis. Differences in network measures between MDD and HC groups were then placed in the corresponding permutation distribution and p values were calculated based on their percentile positions (30,41). The nonparametric permutation test inherently accounts for multiple comparisons ($p < .05$) (43,44).

Each network metric extracted across the specified density range (.1: .02: .5) is represented by a curve that depicts the changes in network metric as a function of network density (threshold). We used functional data analysis (FDA) (29,45,46) to examine depression-associated differences in these curves. In FDA, each network measure curve is treated as a function $(y = f(x))$, and the sum of differences between groups in y-values is calculated at a range of density. Functional data analysis is more sensitive to differences in the shape of the curves than is an area under the curve analysis (45,46). The permutation analysis was conducted on the FDA results to test the significance of the group differences. We used the Brain Connectivity Toolbox (42) to quantify network measures, the Graph Analysis Toolbox

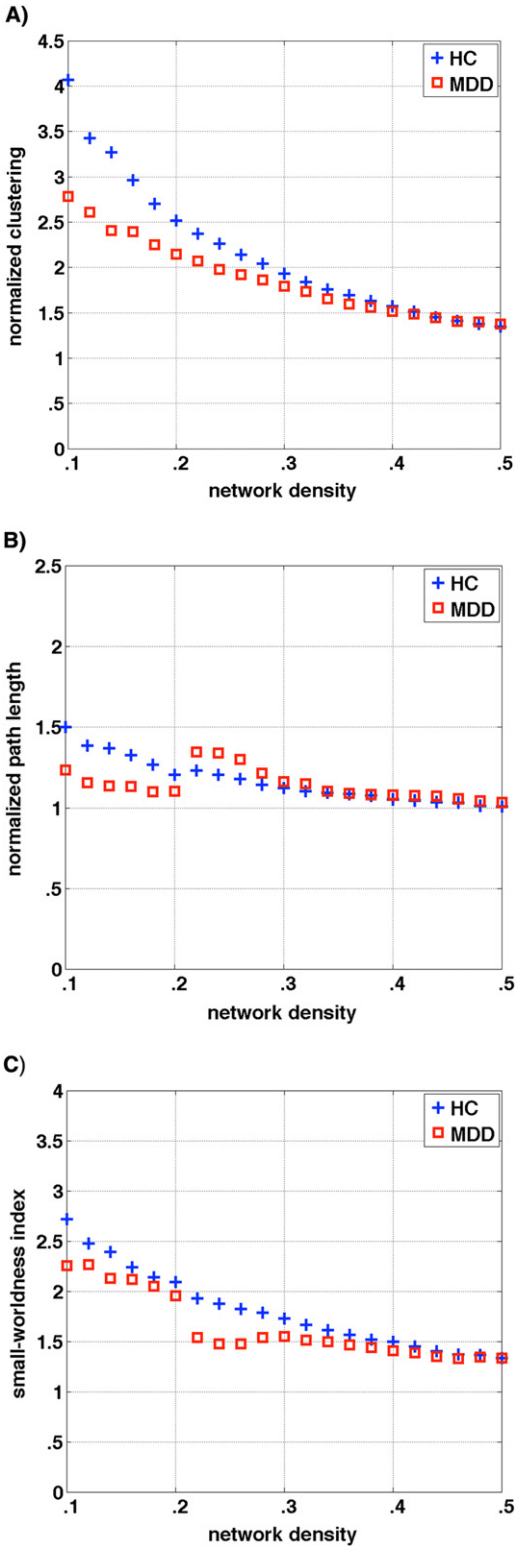

Figure 2. Changes in global network measures as a function of network density. Normalized clustering **(A)**, normalized path length **(B)**, and small-world index **(C)** of the major depressive disorder (MDD) and healthy control (HC) networks.

(29) to compare the structural networks of depressed and nondepressed participants, and the Brain Net Viewer (http://www.nitrc.org/projects/bnv/) for network visualization.

Results

Participant characteristics are summarized in Table 1. Depressed individuals were significantly older and had a higher mean Beck Depression Inventory-II score than HCs ($p < .001$). There were no differences in age among participants run on the three scanners within either the MDD ($F_2 = 1.30$, $p = .28$) or the HC ($F_2 = .56$, $p = .57$) groups.

Global Network Analyses

Structural connectivity matrices computed for each participant were compared both within and between groups to examine differences in global structural network measures of integration (characteristic path length, *L*), local interconnectivity (clustering coefficient, *C*), and the balance of integration and interconnectivity (small-world index, *SW*). Within each group, the minimum network density in which all nodes became connected in the networks was .1. The networks in both the MDD and HC groups followed a small-world organization across the range of densities; that is, *L* of the networks was close to 1, while *C* was higher than 1. This pattern resulted in $SW > 1$ across the range of network densities in both groups (Figure 2).

We examined group differences in global network measures thresholded at a range of densities (.1: .02: .5). The MDD and HC groups differed in global network properties across a range of network densities (Figure 3). Specifically, the networks of the MDD participants had significantly smaller clustering across a number of density thresholds. In addition, MDD participants had significantly smaller small-worldness and longer path lengths than did HCs at densities between .2 and .3 (all $p < .05$).

The FDA analysis ensured that MDD-HC differences in global network measures were not driven by differences in correlation strengths in regional gray matter volumes that would make the analysis less sensitive to thresholding. The results confirmed that MDD participants had significantly smaller normalized clustering ($p = .01$); the two groups did not differ significantly in small-worldness ($p = .1$) or path length $p = .26$). Analyses of nonnormalized network measures also indicated that clustering was significantly smaller in MDD than in HC participants ($p = .04$); the two groups did not differ significantly in path length ($p = .18$).

Regional Network Analyses

Figure 4 presents MDD and HC group hub network layouts mapped on ICBM152 surface templates. Whereas the 20 network hubs identified in the HC group were in frontal executive control and motor regions, the 16 hubs identified in the MDD group were primarily in medial frontal and medial temporal areas. Major depressive disorder participants had higher nodal betweenness than did HCs in the right amygdala and left medial orbitofrontal gyrus and higher nodal degree in the left supramarginal gyrus and right gyrus rectus (Figure 5).

Discussion

This is the first study to use graph analyses to compare gray matter volume correlation networks of depressed and nondepressed adults. Although the networks in both groups followed a

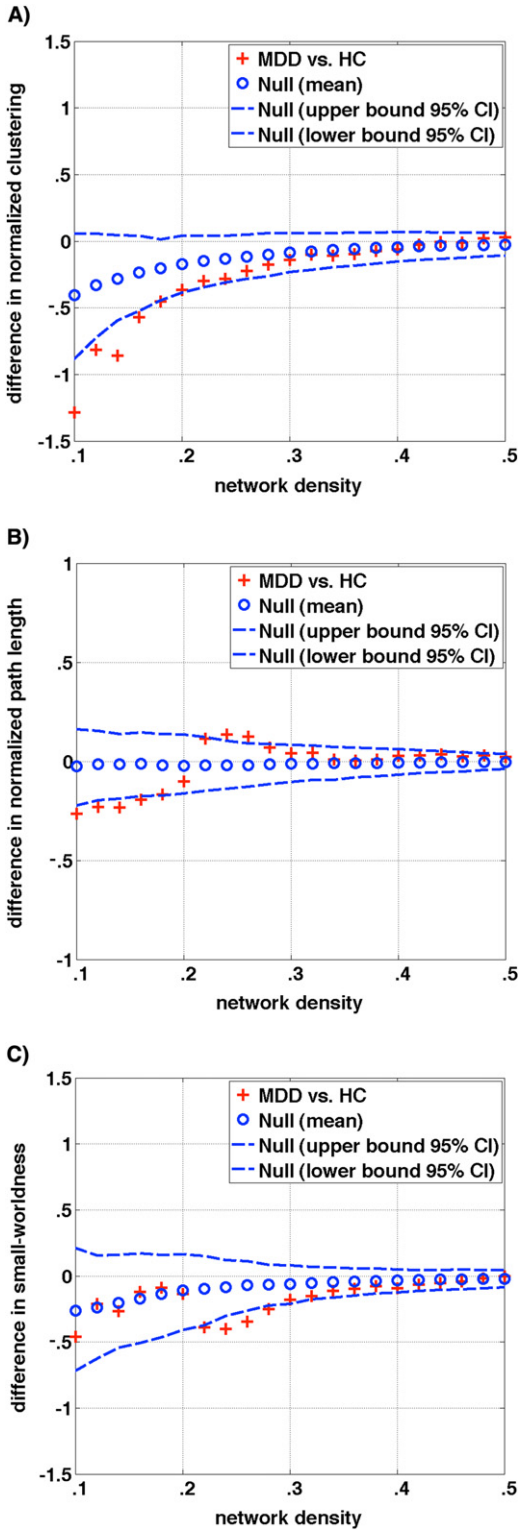

Figure 3. Differences between major depressive disorder (MDD) and healthy control (HC) participants in global network measures as a function of network density. The 95% confidence intervals (CI) and group differences in normalized clustering **(A)**, normalized path length **(B)**, and small-world index **(C)**. The + marker shows the difference between the MDD and HC groups; the + signs falling outside of the confidence intervals indicate the densities in which the difference is significant at $p < .05$. The positive values show MDD > HC and negative values show MDD < HC.

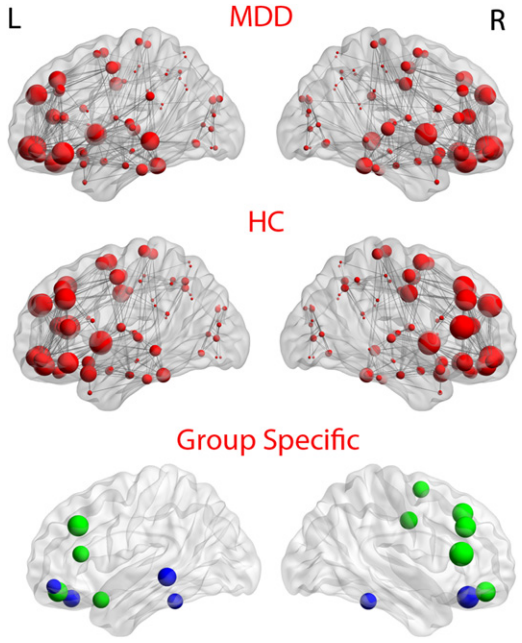

Figure 4. Network hubs. Constructed networks and corresponding hubs for major depressive disorder (MDD) (top) and healthy control (HC) (middle) groups. Nodes that are labeled represent network hubs. The volume of the spheres represents the degree of the corresponding brain region. The bottom panel shows the hubs that are specific to each group. Hubs that were common in the networks of the MDD and HC groups included bilateral medial and inferior orbitofrontal gyrus, left (L) superior frontal gyrus, bilateral superior medial frontal gyrus, right (R) anterior cingulate, and bilateral insula. Hubs present only in the MDD network included the L middle orbitofrontal gyrus, bilateral fusiform, bilateral gyrus rectus, and L middle temporal gyrus. Hubs that were specific to the HC network included R middle cingulate, bilateral inferior frontal triangular gyrus, bilateral middle frontal gyrus, bilateral superior orbitofrontal gyrus, R superior frontal gyrus, R supplemental motor area, and L superior temporal pole. Green color highlights hubs specific to HC network and blue color represents hubs specific to MDD network.

small-world organization across a range of densities, we found alterations of large-scale brain network organization in MDD, even after controlling for total brain volume, gender, age, and scanner field strength. Specifically, we found that, in contrast to healthy control subjects, depressed individuals were characterized by less specialized or segregated network organization, indexed by significantly lower clustering, such that regions were not joining other regions to form a clique of densely interconnected neighbors (16). Importantly, reduced clustering was found in regions that have been implicated in dysfunction of emotion regulation and cognition in MDD (3–5). Our findings suggest that MDD is associated with reduced capacity for subregions of the prefrontal cortex, striatum, and medial temporal cortex to form cliques with other brain regions that are likely to be associated with the generation of such symptoms of depression as persistent sadness, guilt, worthlessness, and recurrent reflective self-focus (16,47). Thus, the network-level aberrations identified in the present study may have important neurobiological implications for the pathophysiology of MDD.

Depression-Associated Anomalies in Global Network Topology

Given our finding of decreased clustering coefficients in MDD, it appears that structural correlation networks in depressed adults are characterized by weaker regional connectivity than is the case in HCs (38). Several investigators have demonstrated that depressed individuals exhibit anomalous patterns of neural connectivity as they engage in cognitive (48) and affective (49) tasks. Most current analytic procedures, however, are limited in their ability to examine relations among regions in whole-brain networks, focusing instead on single regions or on task- or function-specific findings. In the case of MDD, normative function appears to be perturbed by altered network configuration; this anomaly may be a stable characteristic of depression or an adaptation to depressive symptomatology. Decreased clustering in MDD suggests anomalies in coordinated patterns of brain morphology that make up the structural network of depressed individuals.

Morphometric correlations demonstrated by graph analysis reflect connectivity between gray matter regions (17). Importantly, gray matter regions are connected by white matter axons, and both are believed to be influenced by common developmental, trophic, and maturational effects (17,30,50). Cortical dysfunction in one region may result in distant cortical deficits due to primary and/or secondary hodological mechanisms that reflect integrity of underlying white matter pathways (51,52). Thus, the observed differences between depressed and healthy participants in network-level gray matter may be due to neighboring white matter damage in MDD. Indeed, microstructural white matter damage has been documented in MDD (53,54). Interestingly, most of these studies—even those that take a whole-brain statistical approach—identify focal rather than diffuse white matter deficits, particularly in frontosubcortical tracts that are involved in emotion regulation. Inconsistencies in the results of studies have been attributed to disease severity (53) or possible comorbidities of other disorders with depression, such as anxiety (54). One recent study examined white matter structural networks in remitted geriatric depression (55). The investigators found that older individuals with remitted depression had disrupted global network properties, including significantly reduced network strength, decreased global efficiency, and increased absolute path length compared with control subjects. These findings suggest that depressed individuals have sparse connectivity, reduced white matter integrity, and reduced global integration of whole-brain white matter networks due to disconnections between brain regions. Our data also suggest that depression adversely affects global network organization, perhaps explaining why structural anomalies in MDD are more subtle than are conventional radiologically defined abnormalities but are still detectable at a group level (56). Moreover, the wide distribution of structural abnormalities found in MDD suggests that depression affects functionally integrated circuits rather than one or more discrete brain regions (57).

Depression-Associated Anomalies in Regional Network Measures

We used regional network measures, including betweenness and degree, to help localize global network differences between the MDD and HC groups. Nodes with high structural degree and betweenness suggest regions that are highly interactive and that have the potential to participate in a large number of functional interactions (58). In this context, the present findings indicate that there are fewer highly interactive nodes in networks of depressed than of control participants and further that the regions that have high betweenness in MDD (the amygdala, orbital, and medial prefrontal cortical regions) may play a role in maintaining or adapting to depressive pathology.

Other researchers have implicated the amygdala and ventral prefrontal regions in the pathophysiology of depression (59,60).

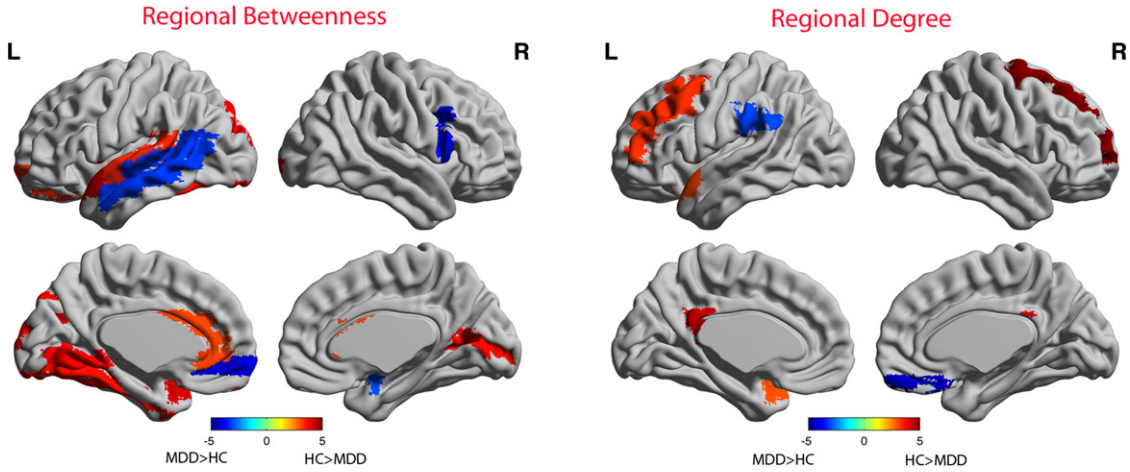

Figure 5. Differences between major depressive disorder (MDD) and healthy control (HC) participants in regional network topology. Regions that showed significant differences between MDD and HC participants in regional betweenness (left panel) and regional degree (right panel) for networks thresholded at minimum density of full connectivity mapped on ICBM152 surface template. The color bar represents *log(1/p value)*. Hot colors in the color bar represent regions that have significantly higher nodal betweenness or degree in the HC than in the MDD, while cold colors denote regions with significantly higher nodal betweenness or degree in the MDD than in the HC. The MDD group showed significantly higher betweenness in the right (R) amygdala, R inferior frontal operculum, left (L) medial orbitofrontal gyrus, and L middle temporal gyrus and higher nodal degree in the L supramarginal gyrus and R gyrus rectus. The HC group had higher betweenness in the L anterior cingulate, L superior orbitofrontal gyrus, L superior temporal gyrus, L superior temporal pole, L lingual gyrus, L fusiform gyrus, and R calcarine fissure and higher nodal degree in the L posterior cingulate, L middle frontal, R superior frontal, L superior temporal pole, L putamen, and bilateral thalamus.

In fact, investigators have documented dysfunction in the prefrontal-limbic neural circuit in MDD, especially during emotional processing. This aberrant functioning may be due to impaired top-down connectivity between the DLPFC and the amygdala and increased bottom-up endogenous effective connectivity from the amygdala to the anterior cingulate cortex (61). The sgACC has been a target for deep brain stimulation treatment in refractory cases of MDD (62). Importantly, and consistent with the present findings, modulating sgACC activity by deep brain stimulation affects a constellation of limbic, paralimbic, and dorsal cortical structures that have also been implicated in MDD (63). Differential interactions between ventral prefrontal and limbic regions based on treatment response (64), as well as results from numerous functional neuroimaging studies (65,66), have contributed to the development of neural models of MDD that posit reciprocal interactions between cortical structures that mediate cognition (e.g., DLPFC and inferior parietal cortex) and cortical and subcortical structures that support emotional functions (e.g., anterior insular cortex, amygdala, and hippocampus) (67). These relations among regions also have implications for efficient information processing and suggest that individuals with MDD rely on more distributed and randomized neural resources (20–22) that are inefficient and maladaptive for mood and cognitive functioning.

The MDD and HC participants also differed in the number and distribution of network hubs. Whereas the 20 network hubs found in the HC group were primarily in frontal executive control and motor regions, the 16 hubs identified in the MDD group were primarily in frontal and temporal areas. Similar to the regional network findings described above, this hub analysis supports formulations that intrinsic functional connectivity originating in the inferior orbitofrontal and medial temporal default mode regions is critical for emotional functioning and is frequently found to be aberrant in MDD (68,69). Previous studies have used task-dependent and resting-state neuroimaging data to examine functional relations between regions that were found to be hubs in our structural analysis. Although neural structure and function are not necessarily isomorphic, there is now clear evidence linking indices of functional connectivity with structural connectivity, suggesting that anomalies in the organization of structural brain networks identified in this study have important implications for neural function in MDD (70).

We should note two limitations of this study. First, the cross-sectional nature of this investigation prevented us from directly testing the temporal relation between network anomalies and the severity or course of MDD. Future studies should include longitudinal and functional evaluations of network measures in depressed patients. Second, to maximize power, we included data from individuals who were scanned at three different MRI scanners. Although this may have introduced some variability in our data, it is important to note that equal proportions of MDD and HC data were acquired on each of the three scanners, that we included field strength as a covariate in our analysis, and that there were no significant group differences in gray matter volumes as a function of scanner.

Despite these limitations, the present findings increase our understanding of the neural bases of MDD by demonstrating aberrations in specific network properties in this disorder. Individuals with MDD were characterized by decreased regional connectivity. Preferential sites for regional connectivity within the MDD group coincide with well-established medial prefrontal and medial temporal regions that have been implicated in this disorder. These results contribute new and important insights concerning the neurobiological mechanisms that might underlie deficits in neural functioning in MDD and highlight critical areas for future research concerning the pervasiveness and effects of structural neural anomalies in this debilitating disorder.

This research was supported by the National Institute of Mental Health Grants MH085919 to Dr. Singh and MH59259 to Dr. Gotlib, and National Institutes of Health Director's New Innovator Award 1

DP2 OD004445-01 to Dr. Kesler. Dr. Singh and all the coauthors had full access to all of the data in the study and take responsibility for the integrity of the data and the accuracy of the data analysis.

The authors report no biomedical financial interests or potential conflicts of interest.

1. Culpepper L (2011): Understanding the burden of depression. *J Clin Psychiatry* 72:e19.
2. Gotlib IH, Joormann J (2010): Cognition and depression: Current status and future directions. *Annu Rev Clin Psychol* 6:285–312.
3. Sacher J, Neumann J, Funfstuck T, Soliman A, Villringer A, Schroeter ML (2012): Mapping the depressed brain: A meta-analysis of structural and functional alterations in major depressive disorder. *J Affect Disord* 140: 142–148.
4. Hamilton JP, Siemer M, Gotlib IH (2008): Amygdala volume in major depressive disorder: A meta-analysis of magnetic resonance imaging studies. *Mol Psychiatry* 13:993–1000.
5. Hamilton JP, Furman DJ, Gotlib IH (2011): The neural foundations of major depression: Classical approaches and new frontiers. In: Lopez-Munoz FF, Alamo C, editors. *Neurobiology of Depression*. Boca Raton, FL: Taylor & Francis Group, 57–73.
6. Amico F, Meisenzahl E, Koutsouleris N, Reiser M, Moller HJ, Frodl T (2011): Structural MRI correlates for vulnerability and resilience to major depressive disorder. *J Psychiatry Neurosci* 36:15–22.
7. Shah PJ, Ebmeier KP, Glabus MF, Goodwin GM (1998): Cortical grey matter reductions associated with treatment-resistant chronic unipolar depression. Controlled magnetic resonance imaging study. *Br J Psychiatry* 172:527–532.
8. Cheng YQ, Xu J, Chai P, Li HJ, Luo CR, Yang T, *et al*. (2010): Brain volume alteration and the correlations with the clinical characteristics in drug-naive first-episode MDD patients: A voxel-based morphometry study. *Neurosci Lett* 480:30–34.
9. Korgaonkar MS, Grieve SM, Koslow SH, Gabrieli JDE, Gordon E, Williams LM (2011): Loss of white matter integrity in major depressive disorder: Evidence using tract-based spatial statistical analysis of diffusion tensor imaging. *Hum Brain Mapp* 32:2161–2171.
10. Zeng LL, Shen H, Liu L, Wang L, Li B, Fang P, *et al*. (2012): Identifying major depression using whole-brain functional connectivity: A multivariate pattern analysis. *Brain* 135:1498–1507.
11. Bassett DS, Bullmore E (2006): Small-world brain networks. *Neuroscientist* 12:512–523.
12. Fan Y, Shi F, Smith JK, Lin W, Gilmore JH, Shen D (2011): Brain anatomical networks in early human brain development. *Neuroimage* 54:1862–1871.
13. Iturria-Medina Y, Canales-Rodriguez EJ, Melie-Garcia L, Valdes-Hernandez PA, Martinez-Montes E, Aleman-Gomez Y, Sánchez-Bornot JM (2007): Characterizing brain anatomical connections using diffusion weighted MRI and graph theory. *Neuroimage* 36:645–660.
14. Chen ZJ, He Y, Rosa P, Germann J, Evans AC (2008): Revealing modular architecture of human brain structural networks by using cortical thickness from MRI. *Cereb Cortex* 18:2374–2381.
15. He Y, Chen ZJ, Evans AC (2007): Small-world anatomical networks in the human brain revealed by cortical thickness from MRI. *Cereb Cortex* 17:2407–2419.
16. Bassett DS, Bullmore ET (2009): Human brain networks in health and disease. *Curr Opin Neurol* 22:340–347.
17. Gong G, He Y, Chen Z, Evans A (2012): Convergence and divergence of thickness correlations with diffusion connections across the human cerebral cortex. *Neuroimage* 59:1239–1248.
18. Watts DJ, Strogatz SH (1998): Collective dynamics of 'small-world' networks. *Nature* 393:440–442.
19. Bullmore E, Sporns O (2009): Complex brain networks: Graph theoretical analysis of structural and functional systems. *Nat Rev Neurosci* 10:186–198.
20. Leistedt SJ, Coumans N, Dumont M, Lanquart JP, Stam CJ, Linkowski P (2009): Altered sleep brain functional connectivity in acutely depressed patients. *Hum Brain Mapp* 30:2207–2219.
21. Zhang J, Wang J, Wu Q, Kuang W, Huang X, He Y, Gong Q (2011): Disrupted brain connectivity networks in drug-naive, first-episode major depressive disorder. *Biol Psychiatry* 70:334–342.
22. Jin C, Gao C, Chen C, Ma S, Netra R, Wang Y, *et al*. (2011): A preliminary study of the dysregulation of the resting networks in first-episode medication-naive adolescent depression. *Neurosci Lett* 503:105–109.
23. First MB, Spitzer RL, Gibbon M, Williams JBW (1996): *Structured Clinical Interview for DSM-IV Axis I Disorders-Patient Version (SCID-P)*. New York: New York State Psychiatric Institute, Biometrics Research Department.
24. Beck AT, Steer RA, Brown GK (1996): *Manual for the Beck Depression Inventory-II*. San Antonio, TX: Psychological Corporation.
25. Schnack HG, van Haren NE, Brouwer RM, van Baal GC, Picchioni M, Weisbrod M, *et al*. (2010): Mapping reliability in multicenter MRI: Voxel-based morphometry and cortical thickness. *Hum Brain Mapp* 31: 1967–1982.
26. Wilke M, Holland SK, Altaye M, Gaser C (2008): Template-O-Matic: A toolbox for creating customized pediatric templates. *Neuroimage* 41: 903–913.
27. Ashburner J, Friston KJ (2005): Unified segmentation. *Neuroimage* 26: 839–851.
28. Tzourio-Mazoyer N, Landeau B, Papathanassiou D, Crivello F, Etard O, Delcroix N, *et al*. (2002): Automated anatomical labeling of activations in SPM using a macroscopic anatomical parcellation of the MNI MRI single-subject brain. *Neuroimage* 15:273–289.
29. Hosseini SM, Hoeft F, Kesler SR (2012): Gat: A graph-theoretical analysis toolbox for analyzing between-group differences in large-scale structural and functional brain networks. *PLoS One* 7:e40709.
30. Bernhardt BC, Chen Z, He Y, Evans AC, Bernasconi N (2011): Graph-theoretical analysis reveals disrupted small-world organization of cortical thickness correlation networks in temporal lobe epilepsy. *Cereb Cortex* 21:2147–2157.
31. He Y, Dagher A, Chen Z, Charil A, Zijdenbos A, Worsley K, *et al*. (2009): Impaired small-world efficiency in structural cortical networks in multiple sclerosis associated with white matter lesion load. *Brain* 132: 3366–3379.
32. Zalesky A, Fornito A, Bullmore E (2012): On the use of correlation as a measure of network connectivity. *Neuroimage* 60:2096–2106.
33. Rubinov M, Sporns O (2011): Weight-conserving characterization of complex functional brain networks. *Neuroimage* 56:2068–2079.
34. van Wijk BCM, Stam CJ, Daffertshofer A (2010): Comparing brain networks of different size and connectivity density using graph theory. *PLoS One* 5:e13701.
35. Maslov S, Sneppen K (2002): Specificity and stability in topology of protein networks. *Science* 296:910–913.
36. Milo R, Shen-Orr S, Itzkovitz S, Kashtan N, Chklovskii D, Alon U (2002): Network motifs: Simple building blocks of complex networks. *Science* 298:824–827.
37. Hirschberger M, Qi Y, Steuer RE (2004): Randomly generating portfolio-selection covariance matrices with specified distributional characteristics. *Eur J Oper Res* 177:1610–1625.
38. Rubinov M, Sporns O (2010): Complex network measures of brain connectivity: Uses and interpretations. *Neuroimage* 52:1059–1069.
39. Hosseini SMH, Black JM, Soriano T, Bugescu N, Martinez R, Raman MM, *et al*. (2013): Topological properties of large-scale structural brain networks in children with familial risk for reading difficulties. *Neuroimage* 71:260–274.
40. Hosseini SMH, Koovakkattu D, Kesler SR (2012): Altered small-world properties of gray matter networks in breast cancer. *BMC Neurol* 12:28.
41. Bassett DS, Bullmore E, Verchinski BA, Mattay VS, Weinberger DR, Meyer-Lindenberg A (2008): Hierarchical organization of human cortical networks in health and schizophrenia. *J Neurosci* 28: 9239–9248.
42. He Y, Chen Z, Evans A (2008): Structural insights into aberrant topological patterns of large-scale cortical networks in Alzheimer's disease. *J Neurosci* 28:4756–4766.
43. Nichols TE, Holmes AP (2001): Nonparametric permutation tests for functional neuroimaging: A primer with examples. *Hum Brain Mapp* 15:1–25.
44. Nichols TE, Hayasaka S (2003): Controlling the familywise error rate in functional neuroimaging: A comparative review. *Stat Methods Med Res* 12:419–446.
45. Bassett DS, Nelson BG, Mueller BA, Camchong J, Lim KO (2012): Altered resting state complexity in schizophrenia. *Neuroimage* 59: 2196–2207.
46. Ramsay JO, Silverman BW (2005): *Functional Data Analysis*. New York: Springer.

47. Menon V (2011): Large-scale brain networks and psychopathology: A unifying triple network model. *Trends Cogn Sci* 15:483–506.
48. Desseilles M, Schwartz S, Dang-Vu TT, Sterpenich V, Ansseau M, Maquet P, Phillips C (2011): Depression alters ''top-down'' visual attention: A dynamic causal modeling comparison between depressed and healthy subjects. *Neuroimage* 54:1662–1668.
49. Carballedo A, Scheuerecker J, Meisenzahl E, Schoepf V, Bokde A, Moller HJ, *et al*. (2011): Functional connectivity of emotional processing in depression. *J Affect Disord* 134:272–279.
50. Catani M, ffytche DH (2005): The rises and falls of disconnection syndromes. *Brain* 128:2224–2239.
51. Catani M, Dell'acqua F, Bizzi A, Forkel SJ, Williams SC, Simmons A, *et al*. (2012): Beyond cortical localization in clinic-anatomical correlation. *Cortex* 48:1262–1287.
52. Zhang K, Sejnowsky TJ (2000): A universal scaling law between gray matter and white matter of cerebral cortex. *Proc Natl Acad Sci U S A* 97:5621–5626.
53. Wu F, Tang Y, Xu K, Kong L, Sun W, Wang F, *et al*. (2011): White matter abnormalities in medication-naive subjects with a single short-duration episode of major depressive disorder. *Psychiatry Res* 191:80–83.
54. Blood AJ, Iosifescu DV, Makris N, Perlis RH, Kennedy DN, Dougherty DD, *et al*. (2010): Microstructural abnormalities in subcortical reward circuitry of subjects with major depressive disorder. *PLoS One* 5:e13945.
55. Bai F, Shu N, Yuan Y, Shi Y, Yu H, Wu D, *et al*. (2012): Topologically convergent and divergent structural connectivity patterns between patients with remitted geriatric depression and amnestic mild cognitive impairment. *J Neurosci* 32:4307–4318.
56. Mwangi B, Ebmeier KP, Matthews K, Steele JD (2012): Multi-centre diagnostic classification of individual structural neuroimaging scans from patients with major depressive disorder. *Brain* 135:1508–1521.
57. Fang P, Zeng LL, Shen H, Wang L, Li B, Liu L, Hu D (2012): Increased cortical-limbic anatomical network connectivity in major depression revealed by diffusion tensor imaging. *PLoS One* 7:e45972.
58. Sporns O (2011): The human connectome: A complex network. *Ann N Y Acad Sci* 1224:109–125.
59. Guilloux JP, Douillard-Guilloux G, Kota R, Wang X, Gardier AM, Martinowich K, *et al*. (2011): Molecular evidence for BDNF- and GABA-related dysfunctions in the amygdala of female subjects with major depression. *Mol Psychiatry* 17:1130–1142.
60. Hamani C, Mayberg H, Stone S, Laxton A, Haber S, Lozano AM (2011): The subcallosal cingulate gyrus in the context of major depression. *Biol Psychiatry* 69:301–308.
61. Lu Q, Li H, Luo G, Wang Y, Tang H, Han L, Yao Z (2012): Impaired prefrontal-amygdala effective connectivity is responsible for the dysfunction of emotion process in major depressive disorder: A dynamic causal modeling study on MEG. *Neurosci Lett* 523:125–130.
62. Mayberg HS, Lozano AM, Voon V, McNeely HE, Seminowicz D, Hamani C, *et al*. (2005): Deep brain stimulation for treatment-resistant depression. *Neuron* 45:651–660.
63. Johansen-Berg H, Gutman DA, Behrens TE, Matthews PM, Rushworth MF, Katz E, *et al*. (2008): Anatomical connectivity of the subgenual cingulate region targeted with deep brain stimulation for treatment-resistant depression. *Cereb Cortex* 18:1374–1383.
64. Pizzagalli DA (2011): Frontocingulate dysfunction in depression: Toward biomarkers of treatment response. *Neuropsychopharmacology* 36:183–206.
65. Hamilton JP, Chen G, Thomason ME, Schwartz ME, Gotlib IH (2011): Investigating neural primacy in major depressive disorder: Multivariate granger causality analysis of resting-state fMRI time-series data. *Mol Psychiatry* 16:763–772.
66. Frodl T, Bokde AL, Scheuerecker J, Lisiecka D, Schoepf V, Hampel H, *et al*. (2010): Functional connectivity bias of the orbitofrontal cortex in drug-free patients with major depression. *Biol Psychiatry* 67: 161–167.
67. Mayberg HS, Liotti M, Brannan SK, McGinnis S, Mahurin RK, Jerabek PA, *et al*. (1999): Reciprocal limbic-cortical function and negative mood: Converging PET findings in depression and normal sadness. *Am J Psychiatry* 156:675–682.
68. Lemogne C, Delaveau P, Freton M, Guionnet S, Fossati P (2012): Medial prefrontal cortex and the self in major depression. *J Affect Disord* 136:e1–e11.
69. Hamilton JP, Furman DJ, Chang C, Thomason ME, Dennis E, Gotlib IH (2011): Default-mode and task-positive network activity in major depressive disorder: Implications for adaptive and maladaptive rumination. *Biol Psychiatry* 70:327–333.
70. Greicius MD, Supekar K, Menon V, Dougherty RF (2009): Resting-state functional connectivity reflects structural connectivity in the default mode network. *Cereb Cortex* 19:72–78.